POLITECNICO
MILANO 1863

SCUOLA DI INGEGNERIA INDUSTRIALE
E DELL'INFORMAZIONE

EXECUTIVE SUMMARY OF THE THESIS

# Optimization of Acid Regeneration in Continuous Ion-Exchange Processes for Nitrogen Removal from Poultry Manure

TESI MAGISTRALE IN FOOD ENGINEERING - INGEGNERIA ALIMENTARE

**AUTHOR: Mozhdeh Abdipour**

**ADVISOR: Fabio Pizzetti**

**ACADEMIC YEAR: 2024-2025**

## 1. Introduction

The growing global demand for energy and the environmental limitations of fossil fuel–based systems have accelerated the transition toward renewable energy sources, with biomass playing a key role due to its availability, carbon-neutral potential, and compatibility with existing infrastructures. Bioenergy remains the largest contributor within the renewable energy sector, supported by agricultural residues and livestock waste, which align with circular bioeconomy principles. Among these resources, poultry manure represents a promising feedstock for anaerobic digestion because of its high organic and nitrogen content. Reported biogas yields range between 0.30 and 0.60 $m^3$ per kg of volatile solids, with methane yields of 0.18–0.35 $m^3$ $CH_4$ $kg^{-1}$ VS and methane concentrations of 55–65% under mesophilic conditions, highlighting its significant potential for sustainable energy production [1].

## 2. Material and Method

Ammonium adsorption–desorption experiments were performed using Amberlyst® 15 resin in a fixed-bed column system operated with a peristaltic pump under controlled flow conditions. Ammonium concentrations were quantified using the indophenol method and UV–Vis spectroscopy at 635 nm, supported by calibration curves prepared from standard solutions. Resin composition and structural integrity were evaluated using CHNS elemental analysis and SEM–EDS, while ICP-OES was employed to quantify $NH_4^+$, $Na^+$, and $K^+$ concentrations in competitive systems to assess selectivity. All experiments were conducted under controlled laboratory conditions using analytical-grade reagents and purified water [2].

### 2.1 Quantification of $NH_4^+$ with indophenol method

The indophenol method, Figure 2.1, was used to quantify ammonium by converting $NH_4^+$ into a blue-colored indophenol complex through reaction with phenol and sodium hypochlorite under alkaline conditions, catalyzed by sodium nitroprusside. After 50 minutes of incubation, the absorbance was measured at 635 nm using UV–Vis spectroscopy, with reagent volumes and concentrations carefully controlled to ensure accurate quantification.

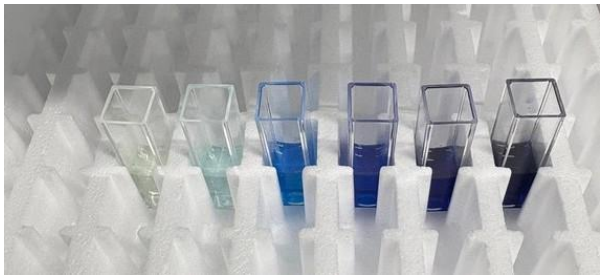

Figure 2.1: Indophenol Method

## 3. Discussion and Result

### 3.1. Quantification of Active Sites by Titration

The titrimetric analysis confirmed the effective activation of Amberlyst® 15 resin. The neutralization of the released $H^+$ ions required 4.7 mL of 1 M NaOH, corresponding to 4.7 mmol of active sites per gram of resin.

Assuming complete ammonium adsorption from a 1000 ppm $NH_4Cl$ solution, this capacity theoretically allows purification of approximately 250 mL of solution per gram of resin. Slight overestimation may occur due to phenolphthalein endpoint detection (pH ≈ 8).

This result confirms that the resin possesses sufficient exchange capacity for the intended adsorption–desorption cycles.

### 3.2. Calibration Curve and Quantification Method

The calibration curve (Figure 3.1) demonstrated a strong linear relationship between absorbance and ammonium concentration within the selected range (15.625–250 ppm). High concentration points (500 and 1000 ppm) were excluded to ensure linearity and analytical accuracy.

The resulting linear equation was used for all concentration calculations in adsorption and desorption experiments, ensuring reliable quantification.

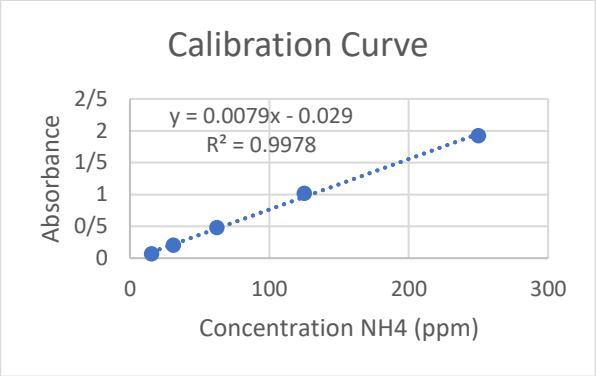


Figure 3.1: Calibration Curve

### 3.3. Optimization of Desorption Conditions

Previous studies identified 0.05 M acid concentration and 20 $mL \cdot min^{-1}$ flow rate as optimal operating conditions. However, excessive acid strength led to extremely rapid desorption, limiting kinetic evaluation and increasing chemical consumption.

Therefore, acid concentrations were progressively reduced to identify the minimum effective regenerant dosage.

### 3.4. Direct Comparison of Acids

#### 3.4.1. Strong Acids vs Weak Acid

The desorption efficiency followed:

$H_2SO_4 \approx HNO_3 >> H_3PO_4$ , as shown in Figure 3.3

$H_2SO_4$ and $HNO_3$ produced sharp initial desorption peaks (~450–500 ppm), confirming rapid and efficient proton exchange.

$H_3PO_4$ showed low, unstable, and incomplete desorption due to its weak dissociation and polyprotic behavior, Figure 3.2.

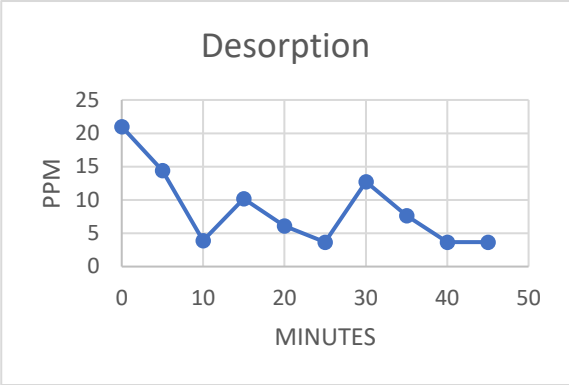


Figure 3.2: Desorption curve with 0.1 M $H_3PO_4$

Considering also its high market price, phosphoric acid was excluded from further evaluation.

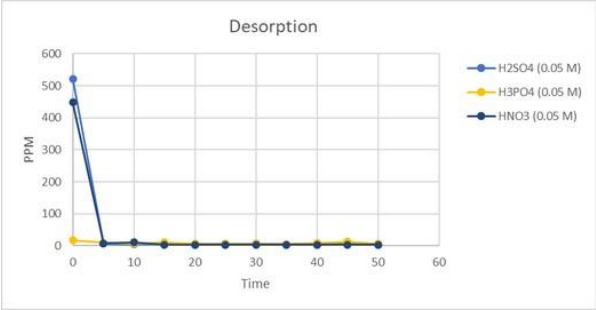


Figure 3.3: Comparison of three acids at the concentration of 0.05 M

## 3.5 Test 1: Ammonium Adsorption from $NH_4Cl$ Solution and Evaluation of Acid Regeneration

Two experiments were performed using columns packed with 1 g of activated resin, each undergoing three consecutive adsorption–desorption cycles. Adsorption was conducted with a 1000 ppm $NH_4Cl$ solution, and desorption was carried out using 0.0125 M $HNO_3$ and $H_2SO_4$ solutions.

### 3.5.1 $NH_4Cl$ and HNO3

Three cycles of adsorption, Figure 3.4, each lasting 50 minutes, were conducted, followed by three cycles of desorption, Figure 3.5, each lasting 45 minutes.

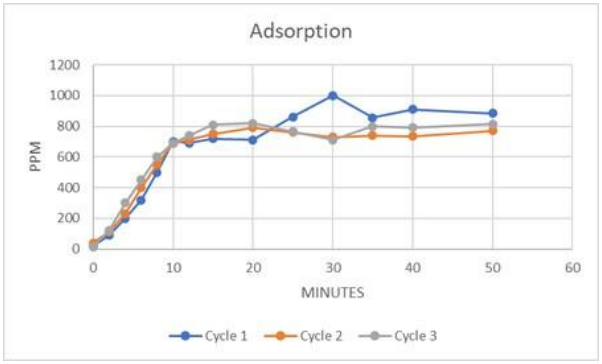


Figure 3.4: Overlapped adsorption cycles

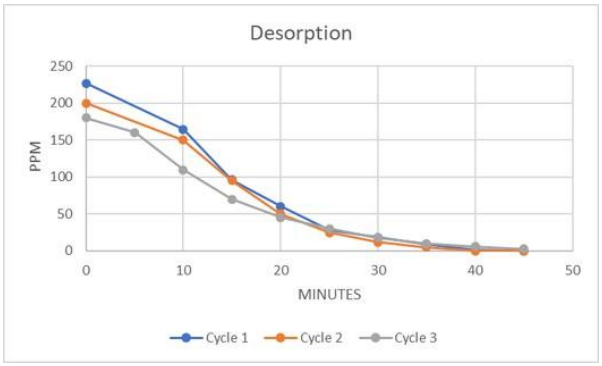


Figure 3.5: Overlapped desorption cycles

The strong overlap of the curves indicates stable adsorption capacity and good reproducibility over repeated cycles. The cycles confirm efficient regeneration and stable resin performance over multiple uses.

### 3.5.2 $NH_4Cl$ and $H_2SO_4$

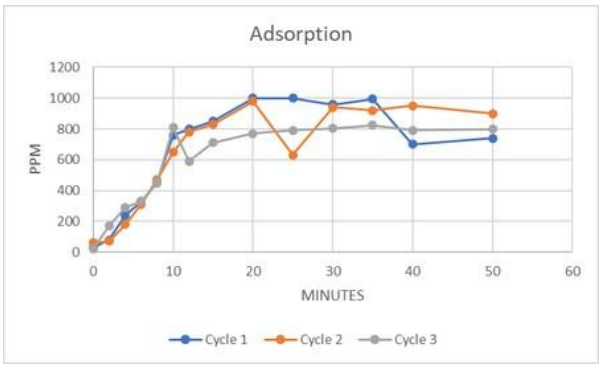


Figure 3.6: Overlapped adsorption cycles

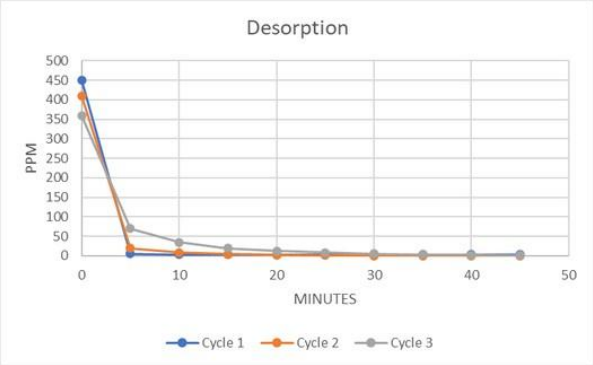


Figure 3.7: Overlapped desorption cycles

The overlapping curves show rapid desorption in Figure 3.7, to near-zero levels, confirming efficient regeneration and stable resin performance over three cycles.

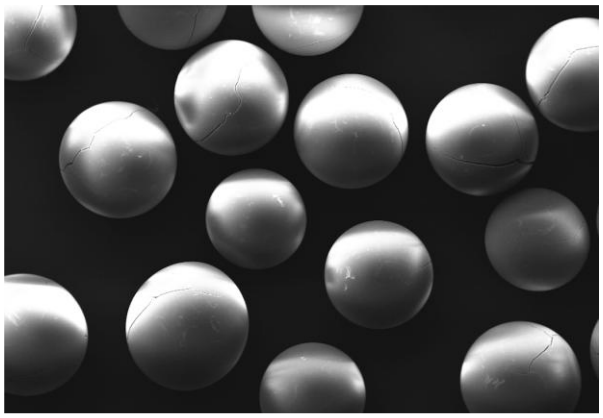

Figure 3.8: Resin before adsorption and desorption cycles

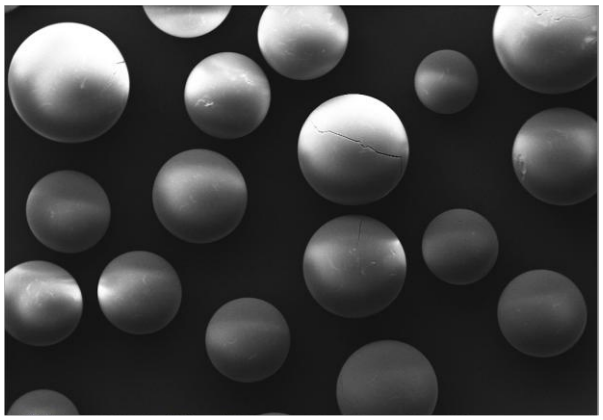

Figure 3.9: Resin after adsorption of $NH_4Cl$ and desorption

As depicted in Figure 3.8 and Figure 3.9, SEM analysis was performed to evaluate the structural integrity of the resin after repeated adsorption–desorption cycles and to detect any possible physical damage.

After three adsorption–desorption cycles, no significant surface damage was observed compared to the activated resin, indicating that the resin maintains its structural integrity.

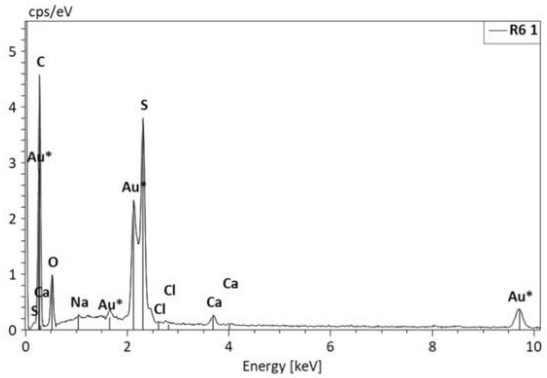


Figure 3.10: EDS spectrum after the adsoprtion and desorption cycles

EDS analysis as shown in Figure 3.10 confirmed the absence of nitrogen after three adsorption–desorption cycles, indicating effective removal of ammonium during regeneration. The minor calcium peaks observed in the spectrum of the resin after the cycles are likely attributable to trace contamination from water rather than to the adsorption process itself.

## 3.6 Test 2: Competitive Desorption in a Ternary Solution of Ammonium, Sodium, and Potassium Chlorides

Despite the presence of competing potassium and sodium ions, the adsorption curves exhibit a consistent and well-defined trend across the cycles, Figure 3.11.

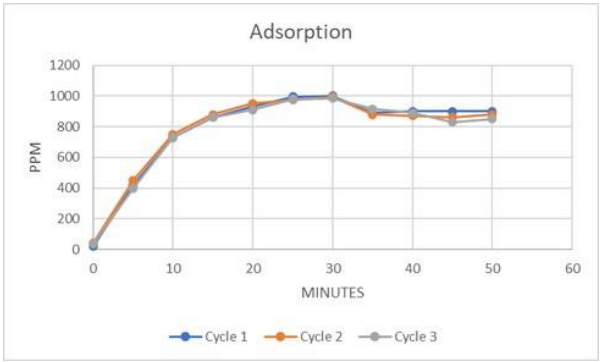


Figure 3.11: Overlapped adsorption cycles with mixed soulution

Pure ammonium shows a rapid increase and a stable high plateau, indicating strong adsorption and delayed breakthrough. In the mixed-salt system, the plateau is slightly lower and stabilization occurs earlier due to competition from $Na^+$ and $K^+$ ions, which reduces the effective ammonium adsorption capacity.

### 3.6.1 Desorption of $HNO_3$

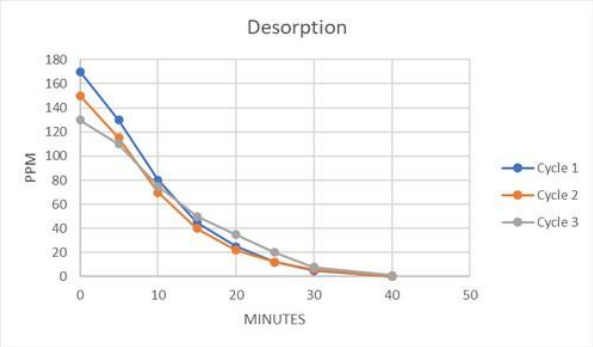


Figure 3.12: Overlapped desorption cycles of $HNO_3$

### 3.6.2 Desorption of $H_2SO_4$

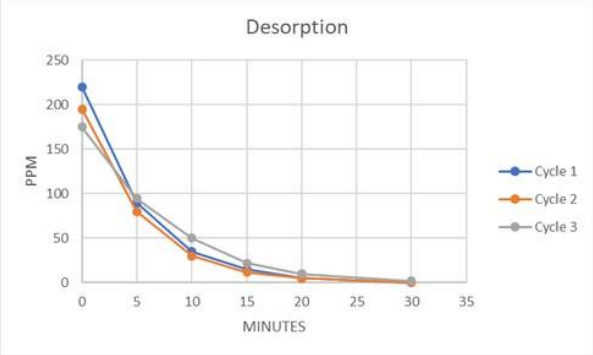


Figure 3.13: Overlapped desorption cycles of $H_2SO_4$

Both curves Figure 3.12 and 3.13 show rapid ammonium removal followed by a gradual decline to near-zero values. However, Figure 3.13 exhibits a higher initial peak and faster regeneration, while Figure 3.12 shows a slightly more gradual desorption behavior.

In the second test, the SEM–EDS elemental mapping, Figure 3.14 confirms the presence of competing cations ($K^+$ and $Na^+$) distributed across the surface, also it showed that the resin particles, even after exposure to the ammonium chloride, potassium chloride and sodium chloride solution, did not exhibit significant structural damage after three cycles.

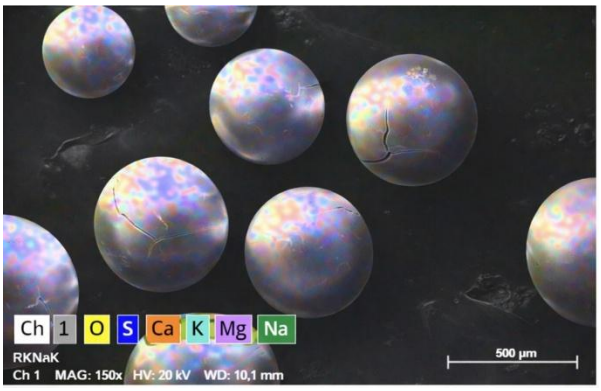


Figure 3.14: EDS mapping of the resin after the adsorption with a solution containing ammonium chloride, potassium chloride and sodium chloride

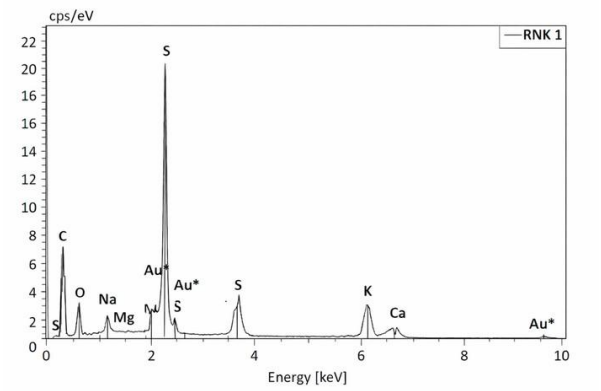


Figure 3.15: EDS spectrum after the three adsorption and desorption cycles in the test with adsoprtion solution containing ammonium chloride, potassium chloride and sodium chloride

As shown in Figure 3.15 minor Mg and Ca peaks were detected, likely due to trace water contamination rather than the ion-exchange process. A small K signal indicates partial potassium retention after desorption, while Na presence was negligible. Surface mapping confirmed complete ammonium removal and minimal competing ion retention, and the Au peaks were attributed to SEM sample preparation.

## 3.7 Market Price

Economic factors are critical in selecting regenerating agents for large-scale ammonium recovery. Among the acids evaluated, sulfuric acid

($H_2SO_4$) exhibits the lowest and most stable market price due to its large-scale production and widespread availability, making it the most suitable option for industrial application. Although hydrochloric acid (HCl) is relatively inexpensive, its high corrosivity can increase operational and maintenance costs. Nitric acid ($HNO_3$) is more expensive due to energy-intensive production, while phosphoric acid ($H_3PO_4$) represents the highest cost and limited economic viability, particularly given its lower regeneration efficiency. Overall, sulfuric acid emerges as the most economically favorable regenerating agent Figure 3.16 [3][4][5].

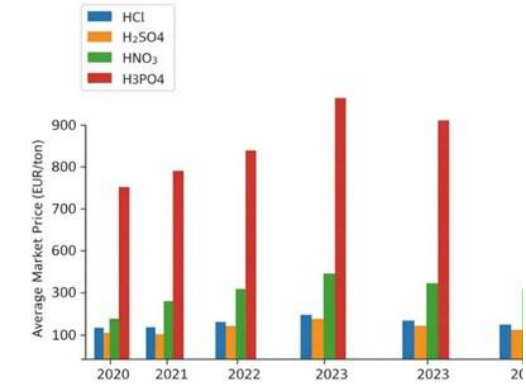


Figure 3.16: Indicative EU Bulk Market Prices of Mineral Acids (2020–2024)

[30

## 4. Conclusions and Future development

This thesis developed and evaluated a continuous fixed-bed ion-exchange process for selective ammonium removal from poultry manure to improve nitrogen management and enhance biogas production efficiency. The study focused on optimizing the regeneration stage of Amberlyst 15 resin by comparing sulfuric acid ($H_2SO_4$), nitric acid ($HNO_3$), and phosphoric acid ($H_3PO_4$) under controlled conditions. The results showed that $H_2SO_4$ provided rapid and efficient regeneration, $HNO_3$ achieved effective but more gradual desorption, and $H_3PO_4$ exhibited poor and irregular performance, as confirmed by CHNS, SEM, and EDS analyses. Considering technical efficiency, resin stability, and market price, sulfuric acid emerged as the most suitable regenerating agent for industrial application. Overall, the study demonstrates that optimized acid regeneration significantly enhances the sustainability, scalability, and industrial feasibility of ion-exchange systems for nitrogen recovery from poultry manure, providing a solid foundation for future large-scale implementation.

## 5. Bibliography

[1] Mohammed Antar, Dongmei Lyu, Mahtab Nazari, Ateeq Shah, Xiaomin Zhou, and Donald L. Smith. *Biomass for a sustainable bioeconomy*: An overview of world biomass production and utilization. Renewable and Sustainable Energy Reviews, 139:110691, 2021. doi: 10.1016/j.rser.2020.110691. URL https://doi.org/10.1016/j.rser.2020.110691.

[2] Gavin Towler and Ray Sinnott. *Chemical Engineering Design*, 2nd edition. Elsevier, Oxford, United Kingdom, 2013. ISBN 978-0-08-096659-5.

[3] M. King. Sulfuric acid production and economics. *Chemical Engineering Progress*, 114(6):28–35, 2018.

[4] Jennifer B. Dunn, Jennifer A. Sullivan, and Elgowainy Amgad. Life-cycle assessment of chlor-alkali processes. *Journal of Cleaner Production*, 103:641–650, 2015. doi: 10.1016/j.jclepro.2014.09.030. URL https://doi.org/10.1016/j.jclepro.2014.09.030.

[5] I. Rafiqul, C. Weber, B. Lehmann, and A. Voss. Energy efficiency improvements in ammonia production. *Energy*, 30(13):2487–2504, 2005. doi: 10.1016/j.energy.2004.09.020. URL https://doi.org/10.1016/j.energy.2004.09.020.

## 6. Acknowledgements

I dedicate this thesis to the memory of all those who sacrificed their lives for the freedom of my homeland, Iran.